Wetting of Ceramic Particulates with Liquid Aluminum Alloys: Part II. Study of Wettability

S.-Y. OH, J. A. CORNIE, and K. C. RUSSELL

Wetting phenomena in ceramic particulate/liquid Al-alloy systems were investigated experimentally using a new pressure infiltration technique developed by the authors. Studies were performed on two different ceramic particulates, SiC and B_4C, with four different liquid aluminum alloy matrices, pure Al, Al-Cu, Al-Si, and Al-Mg. Five major variables tested to study wetting phenomena in ceramic/Al-alloy systems were holding time, melt temperature, alloying element, gas atmosphere, and particulate. Metal:ceramic interfaces were investigated with optical microscopy, SEM, EPMA, and Auger Electron Spectroscopy (AES) in order to understand better the wetting process. The threshold infiltration pressure decreased with temperature as well as with pressurization time for all the ceramic/metal systems. A strong correlation was found between the alloying effect on the threshold pressure and the free energy of formation of oxide phase of the alloying element. More reactive alloying elements were more effective in improving wettability. In air atmospheres, the threshold pressure usually increased markedly as a result of a thick oxide layer formation on the liquid front. Compacts of B_4C particulates showed lower threshold pressures than those of SiC particulates. Fracture occurred in a generally brittle manner in infiltrated SiC specimens. AES element profiles on the fracture surfaces showed fast diffusion of Si, and pile-up of C at the metal:SiC boundaries which promoted fracture through the carbon-rich layer. The fracture surfaces of infiltrated B_4C specimens indicated plastic deformation, hence a more ductile failure mode.

I. INTRODUCTION

IN metal matrix composites, the primary function of the reinforcements is to support most of the applied load, while that of the matrix is to bind the reinforcements together and to transmit and distribute the external loads to the individual reinforcements. Good wetting is needed to generate a strong enough interface to allow transfer and distribution of load from the matrix to the reinforcements without failure.

However, the wettabilities of ceramic materials with liquid aluminum alloys are poor, *i.e.*, have wetting angles substantially higher than 90 deg even well above the matrix melting temperature. For such systems, application of pressure alone cannot overcome poor wettability in the practical sense due to void formation in the small channels during solidification and debonding during service. Acceptable wettability is thus one of the most important parameters for successful casting of composites.

We report here on measurements of wettability in a pressure infiltration device developed by us. Materials used for this study include 10 μm SiC and B_4C particulates, and 4 Al-alloys: pure Al, Al-Cu, Al-Si, and Al-Mg. Major experimental variables were holding time, melt temperature, alloying element, and gas atmosphere. The experimental technique for measuring wettability of ceramic particulates was described in the preceding paper.[1]

S.-Y. OH, Research Associate, Department of Materials Science and Engineering, J. A. CORNIE, Principal Research Associate, Energy Laboratory, and K. C. RUSSELL, Professor of Metallurgy and Nuclear Engineering, are with Massachusetts Institute of Technology, Cambridge, MA 02139.

Manuscript submitted October 9, 1987.

II. BACKGROUND

A. *Wetting of Ceramic Materials with Liquid Aluminum Alloys*

The extremely high oxygen affinity of aluminum makes atmosphere control very important in wetting experiments. The free energy of Al_2O_3 formation is so high that oxide formation in liquid aluminum alloy systems cannot be avoided without special treatments.

Studies have also been made on the wetting of SiO_2,[9-12] SiC,[8,13,14] B_4C,[15,16] TiC,[17,18] and TiB_2[17,18] by molten aluminum alloys with the sessile drop test. Generally, experimental results show significant differences in wetting angles which are mostly caused by differing experimental conditions, particularly time and oxide formation. For example, John and Hausner[11] showed that a very low wetting angle of Al on Al_2O_3 could be obtained by maintaining a very low oxygen partial pressure in the system.

In addition to the oxygen partial pressure in the system, holding time and size of liquid metal droplet on the solid substrate may affect the value of wetting angle due to interfacial reactions.

B. *Metal:Ceramic Interfaces*

Since metal matrix composites are often nonequilibrium systems, there may exist a gradient of chemical potential at the metal:ceramic interface which provides a driving force for interfacial reactions during fabrication or high temperature use. Many investigators[3,9,12,13,19,20] have suggested that interfacial reactions can promote metal/ceramic wetting.

Although the marked stability of ceramic phases in metal/ceramic systems normally permits only modest mutual solubilities, even small amounts of dissolution can significantly decrease the solid:liquid interfacial energy.

Adsorption is a surface reaction which is concentration, temperature, and diffusivity dependent. The relationship

between adsorption and temperature, surface energy, and concentration in dilute solutions is given by the Gibbs adsorption equation:

$$\Gamma_B = -\frac{1}{RT}\frac{d\gamma}{d \ln X_B} \quad [1]$$

where Γ_B is the excess solute concentration at the interface, R is the gas constant, T is the temperature, γ is the surface energy, and X_B is the solute mole fraction. Thus, the greater the adsorption, the more the solute tends to lower the surface energy.

Among the chemical reactions at the metal:ceramic interface, reduction-oxidation (redox) reactions are common. The redox reaction can be represented as:

$$A \text{ (metal)} + B \text{ (cation in compound)} = A \text{ (cation in compound)} + B \text{ (metal)}. \quad [2]$$

This reaction is reversible and governed by the change in total free energy of reaction. The formation of such complex compounds as spinels or glasses also occurs frequently at the metal:ceramic interface.

Two major types of interaction occur at the interface between a liquid and a solid phase: (i) physical and (ii) chemical. Bonding forces due to physical interactions are typically the order of several kJ/mole, but the bonding forces due to chemical interactions are in the range between tens and thousands kJ/mole.[21] Physical interactions determine the wettability by nonreactive liquids such as water and organics which have tenths of J/m^2 as surface energies. However, chemical interactions are dominant in reactive systems where liquid phases have several J/m^2 as surface energies, and provide most of the bonding energy.

In aluminum alloy matrix composites, interfacial reaction studies have been conducted mainly on oxide systems, such as Al_2O_3,[5,7,22-25] and SiO_2.[12] Activity in SiC/Al-alloy systems[26-31] has increased rapidly in the past few years.

III. EXPERIMENTAL METHODS

A. *Infiltration*

Particulates of 9.63 μm SiC or 8.89 μm B_4C were compacted to 52 $\pm$1.5 pct dense 0.5 cm by 3 cm cylinders and pressure infiltrated with one of 7 Al-based alloys. A detailed description of the materials and experimental techniques is given in Part I.[1]

B. *Microstructural Analysis*

Samples for optical microscopy were prepared by first mechanically polishing with 600 and 1000 grit emery papers, then for 2 minutes each with 6 and 1 μm diamond pastes. Finally, the specimens were polished with 0.05 μm alumina for 30 seconds. Between polishing steps, each specimen was rinsed with ethyl alcohol and ultrasonically cleaned for 10 minutes. Cu-bearing aluminum alloys, Al-2 pct Cu and Al-4.5 pct Cu, were etched with a solution of 4 g $KMnO_4$ and 2 g NaOH in 1 liter of distilled water for 10 seconds, as suggested by Mortensen *et al.*[32] Other alloys were doubled-etched; with 5 pct HF for 2 to 3 seconds and with same solution as for Al-Cu alloys for 5 seconds. Keller's reagent, a solution of 10 ml HF, 15 ml HCl, 25 ml HNO_3, and 50 ml distilled water, was also used for deep etching.

C. *Fracture Surface Preparation*

Fracture surfaces of infiltrated powder specimens were analyzed with SEM (AMR or Cambridge) and AES. Since an extensive study on the mechanical properties was beyond the scope of the present work, the specimens were fractured simply clamped in a vise and broken by striking with a hammer. Fractured specimens were coated with approximately 200 Å of gold to give a better image in the SEM. The other halves of fracture specimens were used for AES analysis.

D. *Auger Electron Spectroscopy Analysis*

Auger electron spectroscopy (AES), using a Physical Electronics Industries Inc., model 590, was used to investigate the surface chemistry of particulates and of the fracture surfaces.

Particulates were embedded in 1 mm thick indium foil and inserted into the analyzing chamber, which was maintained at a pressure of about 10^{-7} Pa. The Auger electron spectroscope was operated at 5 kV and 100 nA. For Ar sputtering, 2 kV and 30 $\mu A/cm^2$ were used as electron voltage and beam current.

AES analysis was also performed on fractured specimens in order to determine the chemistry of the metal:ceramic interfacial region. After being fractured by a hammer, the specimens were cut to 1.5 mm thickness. The electron beam conditions included a primary beam voltage of 5 kV and beam current of 100 nA. For depth profile, Ar sputtering was conducted normal to the fracture surface at 4 kV and 70 $\mu A/cm^2$.

Depth profiles were obtained by sputtering both in the particulate and in the matrix directions from the fracture surface. The sputtering rate was estimated as 0.1 nm/sec for matrix; the sputtering rates of SiC and B_4C are expected to be much lower.

IV. CHARACTERIZATION OF SPECIMENS

A. *Surface Characterization of Ceramic Particulates*

The AES profiles which were taken from the as-received SiC and B_4C particulates are shown in Figures 1 and 2, respectively. As seen from the concentration profiles, there were no indications of impurities on the surfaces except small amounts of oxygen.

AES results on the surfaces of SiC and B_4C particulates in uninfiltrated regions before and after infiltration experiments are shown in Figures 1 and 2. Before infiltration, each particulate was preheated for 5 minutes at 800 °C in Ar atmosphere. Including 5 minutes of infiltration time, the particulates were heated for a total of 10 minutes. As can be seen in the AES results, oxygen contents on SiC particulates were reduced during the experiment, while oxygen concentrations of B_4C particulates did not change significantly.

AES results of SiC particulates show that the surface of SiC was cleaned, presumably by reaction of SiC and adsorbed O_2, to form gaseous SiO and either CO_2, CO, or C.[13,33]

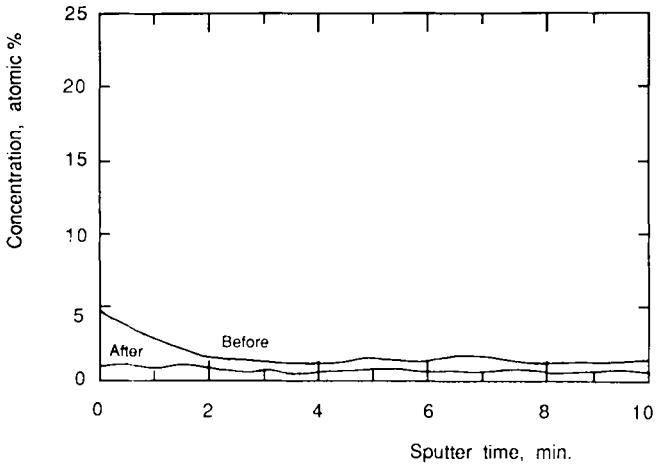

Fig. 1 — AES oxygen concentration profile of SiC particulates before and after infiltration test.

B. *Microstructure of Infiltrated Powder Specimen*

A typical microstructure of a SiC powder compact which was infiltrated with pure Al at 724 kPa is shown in Figure 3. In spite of significant amounts of dissolution of SiC particulates, eutectics were seldom found. The eutectics were absent because the pore size in the compact was smaller than the dendrite tip radius characteristic of our cooling rate. Dendritic solidification was thus impossible and the silicon concentration did not reach the level needed for eutectic formation. However, preferential nucleation of Si phase on the particulate surface was found, in agreement with the earlier observations.[34,35,36]

An electron micrograph of a deep-etched SiC/pure Al specimen is shown in Figure 4. The matrix was dissolved in the concentrated Keller's reagent for 30 seconds. The "bridges" in the microstructure are high-Si phases. The serrated surfaces of particulates are evidence of dissolution of SiC on the high-index planes. The concentration of Si in the matrix was measured as about 5 pct with an electron microprobe analyzer. The probe size was too large to obtain a quantitative measurement of the Si content of the bridges.

Different morphologies in the microstructure of top and bottom portions of SiC/Al-2 pct Si samples indicated that the longer metal:particle contact time for the bottom of the powder specimen which was infiltrated first allowed a higher degree of interfacial reaction. In spite of the large variation in the shape of particulates, the matrix microstructures show only a little difference. In the absence of eutectics one would not expect the matrix appearance to vary much with Si content.

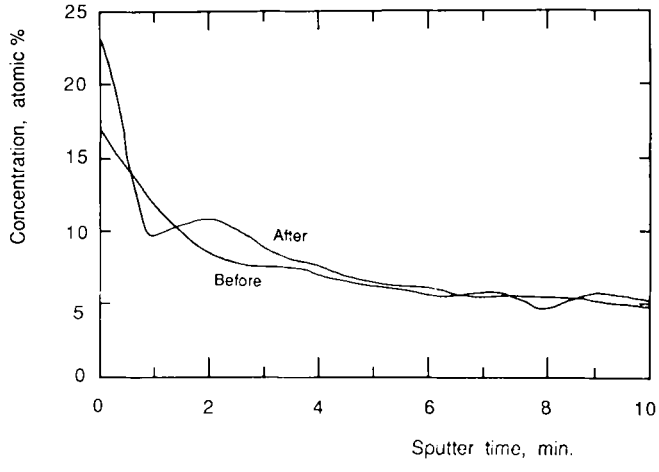

Fig. 2 — AES oxygen concentration profile of B_4C particulates before and after infiltration test.

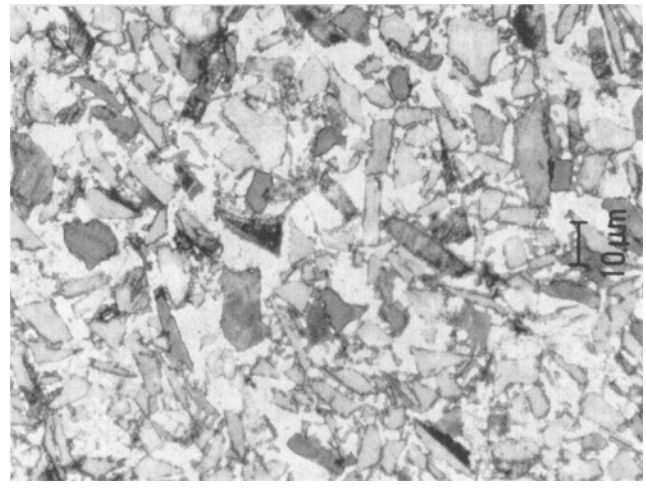

Fig. 3 — Typical microstructure of SiC particulate specimen infiltrated with pure Al at 800 °C.

Since interfacial reaction rate is a strong function of temperature, it is not surprising to see a variation of microstructure with temperature. Figures 5(a) and (b) show the microstructures of SiC specimens infiltrated with pure aluminum at 930 and 634 kPa at 700 °C and 900 °C, respectively. It is obvious that there was much more interfacial reaction at 900 °C.

A typical microstructure of a B_4C powder specimen infiltrated with pure Al at 758 kPa is shown in Figure 6. Because of the extremely high hardness of B_4C particulates, specimen preparation for metallography was not so successful as with SiC.

Generally, microstructures of infiltrated powder specimens showed almost no porosity and a uniform distribution of particulates.

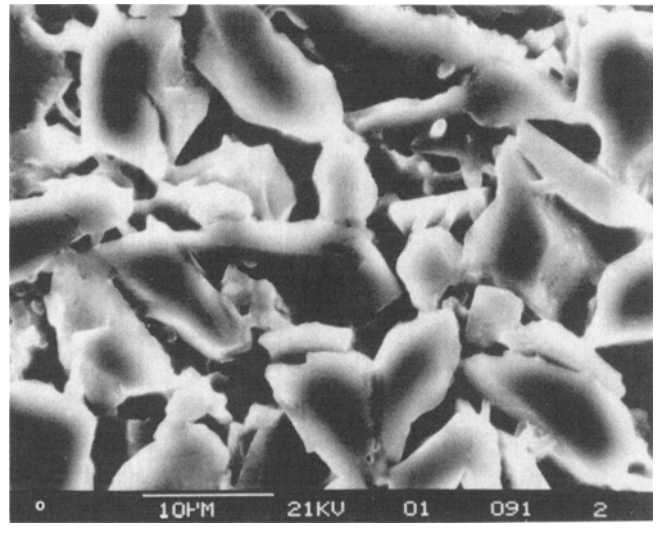

Fig. 4 — SEM micrograph of deep-etched SiC particulate specimen infiltrated with pure Al at 800 °C.

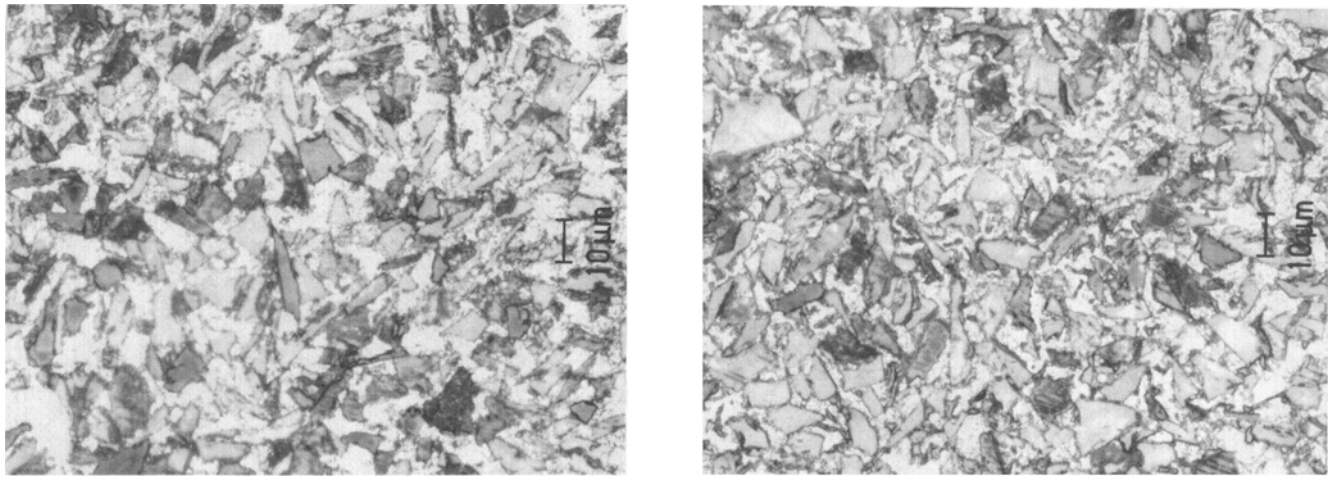

(*a*) (*b*)

Fig. 5—Microstructures of SiC/pure Al system infiltrated at (*a*) 700 °C and (*b*) 900 °C.

C. *Fracture Morphology*

Even though a detailed study of the mechanical properties of infiltrated powder specimens was beyond the scope of the present study, some fracture surfaces of samples broken in bending were examined in order to investigate the metal:ceramic interface. Typical fracture surface morphologies are shown in Figure 7(a) for the SiC/pure Al system, and in Figure 7(b) for the B_4C/pure Al system. The overall fracture morphology of the infiltrated powder specimens was generally unaffected by matrix composition. However, there was a marked difference in the fractographs of different particulate systems, *i.e.*, a more ductile mode in the B_4C/Al-alloy systems. Even though some noninfiltrated regions can be found, debonded interfaces reveal good physical contact between matrix and particulates.

Metal:particulate bonding seems to be weaker for SiC/Al-alloy systems than that of B_4C/Al-alloy systems, as debonding was often found on the fracture surfaces with only a little matrix alloy adhering to the particulate. Fine dimples, indicating ductile fracture, are generally absent from the fracture surface.

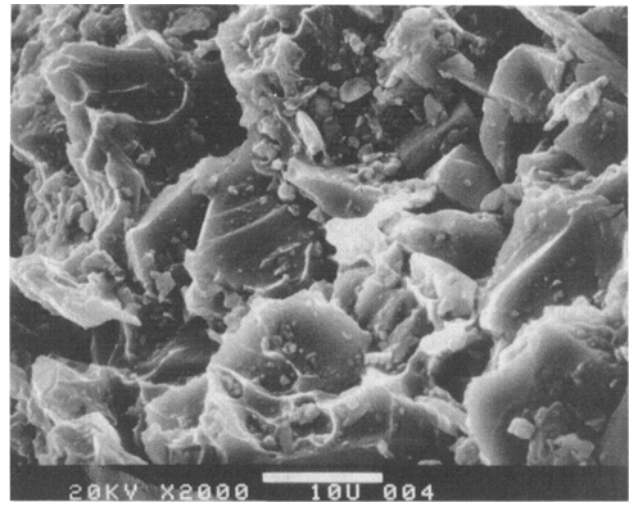

(*a*)

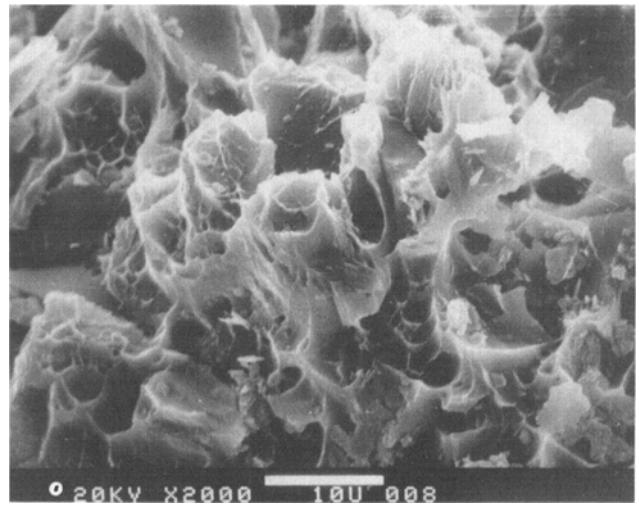

(*b*)

Fig. 7—Fracture surfaces of (*a*) SiC particulate and (*b*) B_4C particulate specimen infiltrated with pure Al at 800 °C.

Fig. 6—Typical microstructure of B_4C particulate specimen infiltrated with pure Al at 800 °C.

For B_4C/Al-alloy specimens, Figure 7(b), most of the fracture surface consists of fine, equiaxed dimples, which is indicative of failure by coalescence of microvoids. The process of microvoid formation and coalescence involves considerable localized plastic deformation and requires the expenditure of a large amount of energy, which is an indication of good fracture toughness. However, irregular fracture surfaces due to fine matrix dimples adhering to the B_4C particulates made AES analysis difficult.

V. WETTING PHENOMENA

A. *Effect of Time*

Change of wettability with time is common in solid ceramic/liquid metal systems because several kinetic processes are often involved. The time dependence of the threshold pressure for wetting in SiC and B_4C particulates with liquid aluminum alloys is shown in Figures 8 and 9. Works of immersion, $W_i = \gamma_{sl} - \gamma_{sv}$, are also shown.

Near-equilibrium wettings were achieved in 5 minutes at 800 °C for SiC with pure aluminum, Al-2 pct Si, and Al-2 pct Mg alloys. However, the threshold pressure decreased almost linearly with time for the Al-2 pct Cu alloy.

The time dependence of wetting may be explained in terms of reaction kinetics in ceramic/metal systems. For a system of high reactivity, metal:ceramic interfacial reactions proceed quickly after physical contact between solid and liquid phases. If the reaction products at the interface are stable both chemically and physically, further reaction will be stopped or retarded significantly. Subsequently, the equilibrium wetting occurs in a short time. However, quick wetting equilibrium can also occur in an inert system which does not involve interfacial reactions, such as a water drop on a platinum plate.

In general, wettability is poor and the wetting process is slow for less reactive systems. Therefore, it takes a longer time to reach an equilibrium wetting. Even though SiC/Al-alloy systems are often regarded as chemically inert,[13] a significant amount of dissolution was observed in the present study, as shown in Figures 3 to 5. The high rate of dissolution of SiC in the liquid Al-alloys can be connected to the high surface-to-volume ratio of particulates as well as high Si solubility in Al.

The Al-2 pct Cu and Al-2 pct Si alloys achieved near-equilibrium wetting of B_4C particulates in 5 minutes. For pure aluminum and Al-2 pct Mg alloys, however, the threshold pressures decreased with time, even after 5 minutes.

Chemical reaction-assisted wetting is expected for B_4C particulates in more reactive alloys, such as Al-2 pct Mg. Liquid boron oxide, B_2O_3, exists on the surface of B_4C above 450 °C[2] and enhances wettability through a liquid-liquid reaction when contacted with liquid metal. Cu or Si in aluminum seems to make this chemical reaction less active, probably due to adsorption of the less reactive element, Cu or Si, at the metal:ceramic interface.

Near-linear decreases of wetting angle with time for the SiC/Al system were observed at 980 °C and 900 °C by Köhler[8] and by Halverson *et al.*,[16] respectively. A linear time dependence of wetting angle was observed in the Al_2O_3/Al system by Brennan and Pask.[3] Achievement of equilibrium wetting in about 5 minutes was reported by

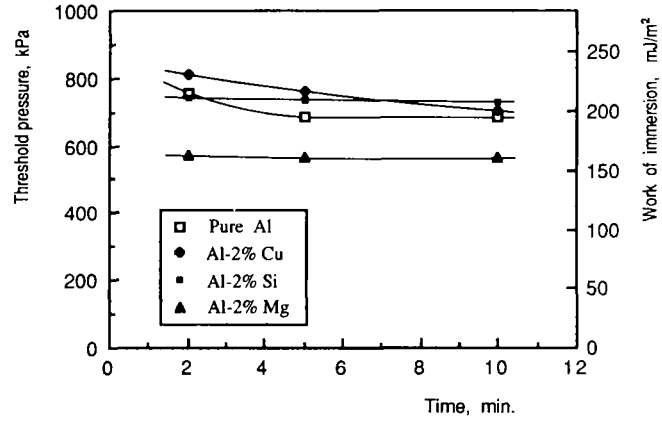

Fig. 8—Change in threshold pressure and work of immersion with time in SiC/Al-alloy systems.

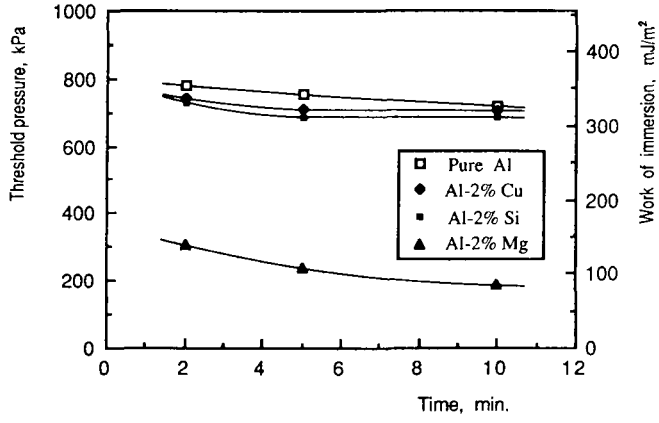

Fig. 9—Change in threshold pressure and work of immersion with time in B_4C/Al-alloy systems.

Samsonov *et al.*[37] for the TiC/Al system at 950 °C, and by Ueki *et al.*[38] for the ZrO_2/Al system at 900 °C.

Breakdown of the oxide layer on the solid ceramic phase either physically or chemically has also been considered as one of the factors affecting the kinetics of wetting.[13,39] Due to the self-cleaning of SiC particulates and liquid oxide layer formation on B_4C particulates, the breakdown of solid oxide films on the ceramic phase is not expected to be a factor in the present systems.

The liquid metal starts infiltration when the applied pressure exceeds the capillary pressure. However, wettability changes with time, mainly due to the reduction of the solid:liquid interfacial energy. If the threshold pressure after time t, $P_{th}(t)$, is smaller than the applied pressure, P_a, infiltration can occur.

Newman's[40] semi-empirical expression for the time dependence of the wetting angle may be applied with minor modification to the time dependence of threshold pressure:

$$P_{th}(t) = P_{th}(eq)[1 + a \cdot \exp(-b \cdot t)] \qquad [3]$$

where $P_{th}(eq)$ is the threshold pressure at equilibrium, and a and b are constants. It was possible to fit our wettability results shown in Figures 8 and 9 to Eq. [3] with constants a, b, and $P_{th}(eq)$ which depend on both matrix composition and particulate type. It is, of course, always possible to fit three data points with a three parameter curve.

B. *Effect of Temperature*

Threshold pressures measured after 5 minutes of holding time for SiC/Al-alloy and B_4C/Al-alloy systems are shown as a function of temperature in Figures 10 and 11, respectively, along with works of immersion. As expected, the threshold pressure decreased with temperature for all the ceramic particulate/Al-alloy systems. This effect is thought to be caused partly by changes in surface energies, and partly by faster interfacial reactions at higher temperature.

Variation of threshold pressure with temperature may be due to the different dominant interfacial reactions or kinetics. In many cases, large increases in wettability were observed at 900 °C for ceramic/Al-alloy systems.[3,8,11,39] This behavior has been explained by both the breakdown of oxide film on the ceramic surface[13,39] and by changes in the oxide layer on the liquid metal surface.[3]

Since complex interfacial reactions are involved in the wetting of these ceramic particulates/liquid aluminum alloy systems, it is natural that each system shows a different relationship between wettability and the temperature. We currently lack the knowledge of the physics and chemistry of interfacial reactions required for a detailed explanation of the temperature dependence of wetting in our ceramic/Al-alloy systems.

C. *Effect of Alloying Elements*

There has been no systematic study on the effect of alloying elements on wetting between ceramic and liquid metal. The alloying elements effective in promoting wetting have been found more or less by trial and error.

Figures 8 to 13 show that Mg is the most effective of the alloying elements tested in promoting wetting of both SiC and B_4C particulates by aluminum alloys. Conversely, Cu and Si had little or no effect on wettability. Magnesium is especially effective in promoting wetting of B_4C. The work of immersion is reduced to 32 mJ/m^2 or, equivalently, the threshold pressure is near zero.

There have been arguments based on the Gibbs adsorption equation, Eq. [2], that small additions of solutes will be sufficient to change the surface energy as long as they can form a monatomic layer at the free surface of liquid or solid:liquid interface. Our experimental results, however, show that the threshold pressure still changes when the solute concentration goes from 2 pct to 4.5 pct.

Liquid aluminum has an extremely high oxygen affinity which makes chemical reactions involving oxygen inevitable at the liquid aluminum:ceramic interface. These interfacial reactions may reduce the interfacial energy of solid ceramic and liquid metal.

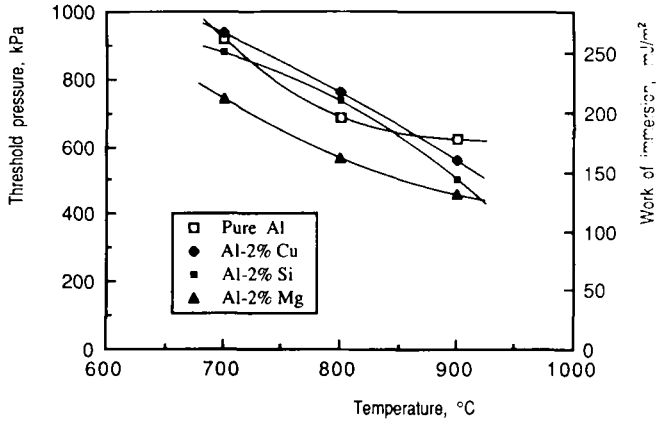

Fig. 10—Change in threshold pressure and work of immersion with temperature in SiC/Al-alloy systems.

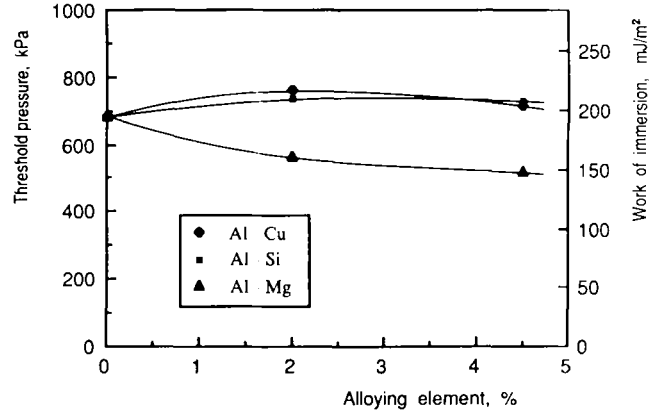

Fig. 12—Change in threshold pressure and work of immersion with alloying element in SiC/Al-alloy systems.

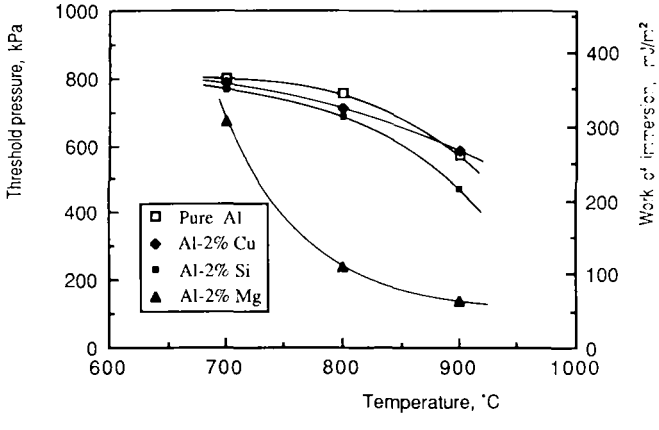

Fig. 11—Change in threshold pressure and work of immersion with temperature in B_4C/Al-alloy systems.

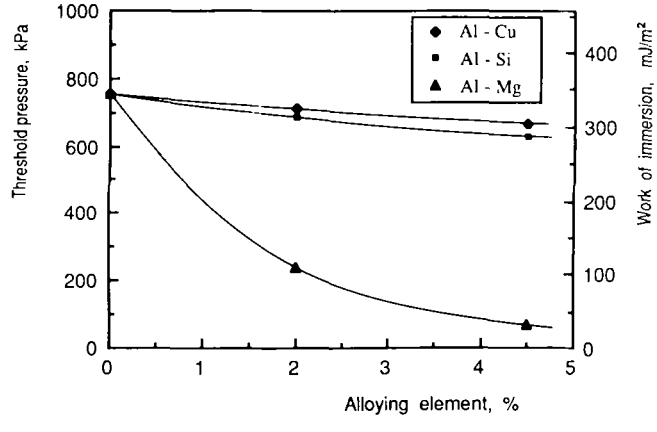

Fig. 13—Change in threshold pressure and work of immersion with alloying element in B_4C/Al-alloy systems.

Figures 14 and 15 show the relationship between the free energy of oxide formation of alloying elements and the threshold pressure for wetting in SiC and B_4C with aluminum alloys. The free energies of Cu_2O, SiO_2, and MgO (per mol of gaseous O_2) were calculated from JANAF Tables[2] for each infiltration temperature. There is a strong correlation between the free energy of oxide formation and the threshold pressure. The larger the negative values of free energy of formation, the lower the threshold pressures are. However, the effectiveness of alloying varied with temperature and ceramic/metal system.

D. *Effect of Gas Atmosphere*

The threshold pressures and works of immersion for SiC/Al-alloy and B_4C/Al-alloy systems in Ar and air atmospheres are listed in Table I. In most cases, the threshold pressure is greater in air than that in Ar.

An air atmosphere is expected to give greater oxidation of particulates and formation of a thicker oxide layer on the surface of the liquid metal. Obviously, the oxide film on the particulates and the oxide layer on the liquid metal surface change the wetting process as well as wettability.

Since SiO_2 has a much lower surface energy, 307 mJ/m^2 1000 °C,[41] than that of SiC, 840 mJ/m^2 at 1200 °C, [39] the wetting angle may increase after oxidation of SiC.

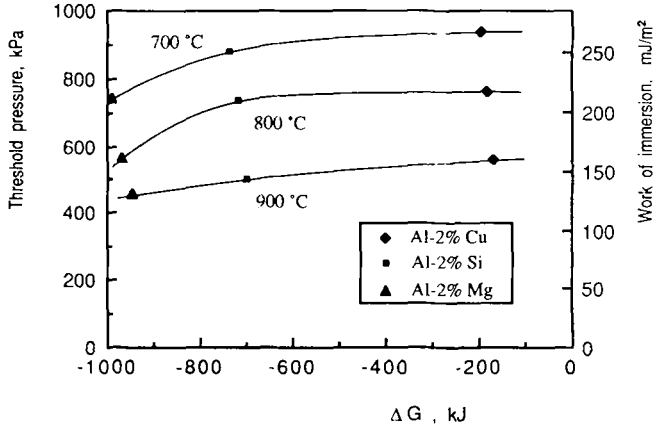

Fig. 14—Relationship between the threshold pressure and free energy of formation of oxide of each alloying element in SiC/Al-alloy systems. Thermodynamic data are from Ref. 2 (per mol O_2); free energies were calculated for each infiltration temperature.

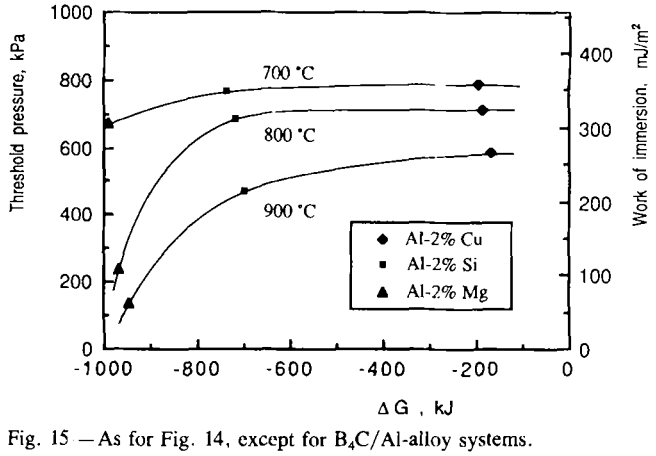

Fig. 15—As for Fig. 14, except for B_4C/Al-alloy systems.

Table I. Threshold Pressure and Work of Immersion for SiC and B_4C Particulates in Ar and in Air Atmospheres at 800 °C

System	In Ar		In Air	
	P_{th} (kPa)	W_i (mJ/m^2)	P_{th} (kPa)	W_i (mJ/m^2)
SiC/pure Al	686	197	710	204
SiC/Al-2 pct Cu	759	218	745	214
SiC/Al-2 pct Si	738	212	779	223
SiC/Al-2 pct Mg	565	162	779	223
SiC/Al-4.5 pct Cu	717	206	807	231
SiC/Al-4.5 pct Si	731	210	731	210
SiC/Al-4.5 pct Mg	524	150	731	210
B_4C/pure Al	752	344	724	332
B_4C/Al-2 pct Cu	710	325	717	328
B_4C/Al-2 pct Si	686	314	738	338
B_4C/Al-2 pct Mg	241	111	69	32
B_4C/Al-4.5 pct Cu	669	306	724	332
B_4C/Al-4.5 pct Si	627	287	655	300
B_4C/Al-4.5 pct Mg	69	32	69	32

Decreased threshold pressures were observed for some B_4C/Al-alloy systems tested in air atmospheres. The decrease in threshold pressure, or increased wettability, is believed to be caused by the formation of a thicker layer of liquid B_2O_3 on the B_4C particulates in an air atmosphere.

VI. INTERFACIAL PHENOMENA

A. *Particulates:Atmosphere Reactions*

Several studies have been conducted on reactions of SiC with gaseous environments. However, information on the reaction of B_4C with gases is scarce. Since the surface characteristics of the solid phase play an important role in wetting, gas-solid reactions should be considered carefully.

The free energies of particulate formation play an important role in interfacial reactions. In spite of some disagreement among different researchers[2,42,43] on SiC, B_4C, and Al_4C_3, it can be estimated that SiC has the most negative value of free energy of formation among the three and that of B_4C has the least, making it the least stable. Unlike their carbides, free energies of formation of oxides for Si, B, and Al are very negative, so that both SiC and B_4C are very prone to oxidation.

The AES results for SiC before and after infiltration experiment, as shown in Figure 1, show that the surface of SiC was cleaned by the reaction of gaseous SiO formation.

The major oxide on the B_4C surface is believed to be B_2O_3 because of its largest negative free energy of formation. Due to its low melting point, 450 °C,[2] B_2O_3 on the surface of particulates exists as liquid during the infiltration test.

B. *Metal:Ceramic Interface*

Ceramic/metal systems are much more stable chemically than metal/metal systems. Therefore, the reactivity at the metal:ceramic interface is usually quite low, generating only a small amount of reaction products. A number of studies[5,7,15,22-29,31,44-53] have been conducted of ceramic:Al-alloy interface phenomena.

The results of Auger analyses performed on a fractured SiC/pure Al specimen obtained by sputtering into the matrix and into the particulate are shown in Figures 16 and 17, respectively. Inside the matrix, the concentration of Al increases rapidly, finally becoming constant. The concentration of C changed in an exactly opposite behavior to Al, as expected. However, the concentration of Si did not change much with sputtering time. This tendency can be explained by fast diffusion of Si after dissolution of SiC particulates, and pile-up of C on the undissolved part of SiC particulates due to its extremely low solubility in Al. Considering the sputtering rate, approximately 0.1 nm/sec, the interfacial region is about 300 Å thick.

In spite of almost zero solubility of B and C in Al, the AES analyses on the fracture surfaces of B_4C/Al-alloy specimens showed similar C profiles as in SiC specimens.

Even though the dissolution of SiC and B_4C were confirmed in various ways, no solid evidence of Al_4C_3 formation was found in the present experiments. This observation may result from the expected extremely small size of Al_4C_3 particles due to short reaction time. Studies[26,29] were made of the reaction of molten aluminum with SiC fibers during short reaction times. Conventional analytic tools including TEM or XRD showed no evidence of Al_4C_3. Of course, large flakes of Al_4C_3 have been found in the case of long thermal exposure.[27,44]

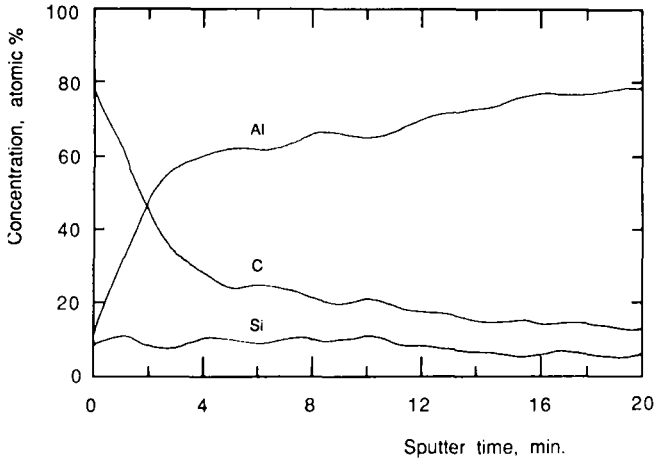

Fig. 16—AES element profile for matrix-side from the fracture surface of SiC/pure Al specimen.

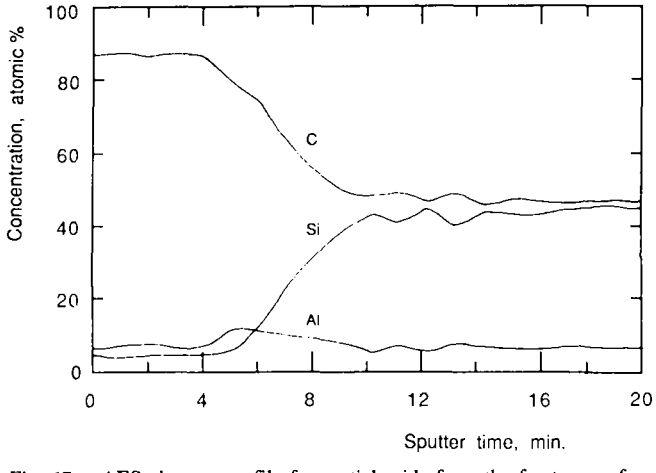

Fig. 17—AES element profile for particle-side from the fracture surface of SiC/pure Al specimen.

In general, dissolution of particulates produced a carbon-rich layer at metal:ceramic boundaries where fracture occurred. Due to its slowness, dissolution is believed to commence after infiltration and therefore has little effect on wettability. However, the liquid layer of B_2O_3 is expected to react quickly with liquid aluminum alloys to form oxide compounds, such as $B_2O_3 \cdot Al_2O_3$ and $B_2O_3 \cdot MgO$ during infiltration.

VII. SUMMARY

Five major variables were tested to study wetting phenomena in ceramic particulate/metal systems. Variables include holding time, melt temperature, solute concentration, gas atmosphere, and particulate. The metal:ceramic interfaces were analyzed with optical microscopy, SEM, EPMA, and Auger electron spectroscopy.

The results of this work are summarized in the following statements:

1. The threshold infiltration pressure decreased exponentially with time for all systems, generally approaching the equilibrium value in 5 minutes.
2. The threshold pressure decreased with increasing temperature, probably due to accelerated kinetics of reactions on the solid:vapor, liquid:vapor, and solid:liquid interfaces.
3. Generally, alloying elements which were strong oxide formers were more effective in improving wettability. Mg alloying decreased the threshold pressure in both particulate systems significantly, and Cu and Si had little effect.
4. Threshold pressures were usually higher in air atmospheres as a result of thick oxide layer formation on the liquid front. The decrease of threshold pressure in B_4C/Al-Mg systems in air atmosphere is connected with the formation of a thicker liquid layer of B_2O_3 on the particulates.
5. B_4C particulates showed lower threshold pressures than SiC particulates due to reaction between liquid B_2O_3 and Al alloy.
6. AES element profiles of infiltrated SiC showed fast diffusion of Si and pile-up of C at the metal:ceramic boundary.
7. Fracture occurred in a more or less brittle manner in infiltrated SiC specimens. However, fracture surfaces of infiltrated B_4C specimens showed small dimples which are an indication of plastic deformation. Generally, fracture occurred through the metal:ceramic interfacial region, especially through the carbon-rich layer, which was present on both particulates.
8. The major interfacial reactions affecting wettability are believed to be dissolution of particulates for SiC and liquid:liquid reaction for B_4C particulates.

ACKNOWLEDGMENTS

The authors are grateful for the financial support provided by the SDIO/ONR under contract number N00014-85-0645. The authors also wish to thank Norton Company for the ceramic particulates.

REFERENCES

1. S.-Y. Oh, J.A. Cornie, and K.C. Russell: *Metall. Trans. A*, 1989, vol. 20A, pp. 527-32.
2. JANAF Thermochemical Tables, 2nd ed., D.R. Stull and H. Prophet, eds., NBS, 1971.
3. J.J. Brennan and J.A. Pask: *J. Am. Ceram. Soc.*, 1968, vol. 51, pp. 569-73.
4. R.D. Carnaham, T.L. Johnston, and C.H. Li: *J. Am. Ceram. Soc.*, 1958, vol. 41, pp. 343-47.
5. J.E. McDonald and J.G. Eberhart: *Trans. AIME*, 1965, vol. 233, pp. 512-17.
6. S.M. Wolf, A.P. Levitt, and J. Brown: *Chem. Eng. Prog.*, 1966, vol. 62, pp. 74-78.
7. J.A. Champion, B.J. Keene, and J.M. Sillwood: *J. Mat. Sci.*, 1969, vol. 4, pp. 39-49.
8. W. Köhler: *Aluminium*, 1975, vol. 51, pp. 443-47.
9. Yu.V. Naidich, Yu.N. Chubashov, N.F. Ishchuk, and V.P. Krasovskii: *Powder Metall. Met. Ceram.*, 1983, vol. 22, pp. 481-83.
10. L. Coudurier, J. Adorian, D. Pique, and N. Eustathopoulos: *Rev. Int. Hautes Tempér. Réfract., Fr.*, 1984, vol. 21, pp. 81-93.
11. H. John and H. Hausner: *J. Mat. Sci. Lett.*, 1986, vol. 5, pp. 549-51.
12. C. Marumo and J.A. Pask: *J. Mat. Sci.*, 1977, vol. 12, pp. 223-33.
13. R. Warren and C.-H. Andersson: *Composites*, April 1984, pp. 101-11.
14. V. Laurent, D. Chatain, and N. Eustathopoulos: *J. Mat. Sci.*, 1987, vol. 22, pp. 244-50.
15. C.R. Manning and T.B. Gurganus: *J. Am. Ceram. Soc.*, 1966, vol. 52, pp. 74-78.
16. D.C. Halverson, A.J. Pyzik, and I.A. Aksay: in *Ceramic Engineering and Science Proceedings*, Am. Ceram. Soc., July-Aug. 1985, pp. 736-44.
17. S.K. Rhee: *J. Am. Ceram. Soc.*, 1970, vol. 53, pp. 386-89.
18. G.A. Yasinskaya: *Sov. Powder Metall. Met. Ceram.*, 1966, vol. 7, pp. 557-59.
19. I.A. Aksay, C.E. Hoge, and J.A. Pask: *J. Phys. Chem.*, 1974, vol. 78, pp. 1178-83.
20. O.B. Kozlora and S.A. Suvorov: *Refractories*, 1976, vol. 17, pp. 763-67.
21. J.V. Naidich: in *Progress in Surface and Membrane Science*, Academic Press, 1981, vol. 14, pp. 353-484.
22. C.G. Levi, G.J. Abbaschian, and R. Mehrabian: *Metall. Trans. A*, 1978, vol. 9A, pp. 697-711.
23. A. Munitz, M. Metzger, and R. Mehrabian: *Metall. Trans. A*, 1979, vol. 10A, pp. 1491-97.
24. I.W. Hall and V. Barrailler: *Metall. Trans. A*, 1986, vol. 17A, pp. 1075-80.
25. G.R. Cappleman, J.F. Watts, and T.W. Clyne: *J. Mat. Sci.*, 1985, vol. 20, pp. 2159-68.
26. A. Skinner, M.J. Koczak, and A. Lawley: in *Proc. of the 5th Annual Conference on Composites and Advanced Ceramic Materials*, J.W. McCauley, ed., Am. Ceram. Soc., 1981, pp. 827-40.
27. S. Towata and S. Yamada: *J. Japan Inst. Met.*, 1983, vol. 47, pp. 159-65.
28. T. Iseki, T. Kameda, and T. Maruyama: *J. Japan Inst. Met.*, 1984, vol. 19, pp. 1692-98.
29. S.R. Nutt and R.W. Carpenter: *Mat. Sci. Eng.*, 1985, vol. 75, pp. 169-77.
30. S.R. Nutt: in *Interfaces in Metal-Matrix Composites*, A.K. Dhingra and S.G. Fishman, eds., AIME, 1986, pp. 157-67.
31. S. Inoue, Y. Okuyama, K. Yoshii, and H. Kawabe: *J. Japan Inst. Met.*, 1987, vol. 51, pp. 5-11.
32. A. Mortensen, M.N. Gungor, J.A. Cornie, and M.C. Flemings: *J. Met.*, March 1986, pp. 30-35.
33. G.L. Humphrey, S.S. Todd, J.P. Coughlin, and E.G. King: Bur. Mines Report Invest., No. 4888, July 1952.
34. T.W. Clyne, M.G. Bader, G.R. Cappleman, and P.A. Hubert: *J. Mat. Sci.*, 1985, vol. 20, pp. 85-96.
35. B.P. Krishnan and P.K. Rohatgi: *Met. Tech.*, 1984, vol. 11, pp. 41-44.
36. P.K. Rohatgi, R. Asthana, and S. Das: *Int. Met. Rev.*, 1986, vol. 31, pp. 115-39.
37. G.V. Samsonov, A.D. Panasyuk, and G.K. Kozina: *Sov. Powder Metall. Met. Ceram.*, 1968, vol. 71, pp. 874-78.
38. M. Ueki, M. Naka, and I. Okamoto: *J. Mat. Sci. Lett.*, 1986, vol. 5, pp. 1261-62.
39. B.C. Allen and W.D. Kingery: *Trans. AIME*, 1959, vol. 215, pp. 30-36.
40. S. Newman: *J. Colloid and Interface Sci.*, 1968, vol. 26, pp. 209-13.
41. S.H. Overbury, P.A. Bertrand, and G.A. Somojai: *Chem. Rev.*, 1975, vol. 75, pp. 547-60.
42. F.D. Richardson: *J. Iron Steel Inst.*, Sept. 1953, pp. 33-51.
43. E.T. Turkdogan: U.S. Steel Company, 1970.
44. S. Towata, S. Yamada, and T. Ohwaki: *Tr. Japan Inst. Met.*, 1985, vol. 26, pp. 563-70.
45. A.E. Standage and M.S. Gani: *J. Am. Ceram. Soc.*, 1967, vol. 50, pp. 101-05.
46. H. Mitani and H. Nagai: *J. Japan Inst. Met.*, 1967, vol. 31, pp. 1296-1300.
47. K. Prabriputaloong and M.R. Piggott: *J. Am. Ceram. Soc.*, 1973, vol. 56, pp. 177-80.
48. K. Prabriputaloong and M.R. Piggott: *J. Am. Ceram. Soc.*, 1973, vol. 56, pp. 184-85.
49. K. Prabriputaloong and M.R. Piggott: *J. Electrochem. Soc.*, 1974, vol. 121, pp. 430-34.
50. R.L. Mehan and D.W. McKee: *J. Mat. Sci.*, 1976, vol. 11, pp. 1009-18.
51. A.S. Isaikin, V.M. Chubarov, B.F. Trefilov, V.A. Silaev, and Yu.A. Gorelov: *Met. Sci. Heat Treatment*, 1980, vol. 22, pp. 815-17.
52. A.M. Stoneham: *Appl. Surf. Sci.*, 1982-83, vol. 14, pp. 249-59.
53. F. Delannay, L. Froyen, and A. Deruyttere: *J. Mat. Sci.*, 1987, vol. 22, pp. 1-16.